arXiv:1510.02992v1 [hep-ex] 10 Oct 2015

DPF2015-393
October 13, 2015

Recent QCD results from the Tevatron

Costas Vellidis

Fermi National Accelerator Laboratory
Batavia, IL 60510, USA

Four years after the shutdown of the Tevatron proton-antiproton collider, the two Tevatron experiments, CDF and DZero, continue producing important results that test the theory of the strong interaction, Quantum Chromodynamics (QCD). The experiments exploit the advantages of the data sample acquired during the Tevatron Run II, stemming from the unique $p\bar{p}$ initial state, the clean environment at the relatively low Tevatron instantaneous luminosities, and the good understanding of the data sample after many years of calibrations and optimizations. A summary of results using the full integrated luminosity is presented, focusing on measurements of prompt photon production, weak boson production associated with jets, and non-perturbative QCD processes.

PRESENTED AT

DPF 2015
The Meeting of the American Physical Society
Division of Particles and Fields
Ann Arbor, Michigan, August 4–8, 2015

1 Introduction

The Tevatron proton-antiproton collider at the Fermi National Accelerator Laboratory (Fermilab) operated at a collision energy of 1.96 TeV (980 GeV per beam) from 2002 through 2011 (Run II) and was the highest-energy machine in the World until 2010, when the LHC proton-proton collider at CERN started operations. At the end of Run II, two short runs were performed at collision energies of 300 and 900 GeV. During Run II, the collider delivered an integrated luminosity of approximately 12 fm^{-1}. The two experiments, CDF and DZero, acquired data corresponding to an integrated luminosity of approximately 10 fm^{-1} each. The two multi-purpose detectors consisted of high-resolution tracker, calorimeter, and muon detection compartments. Both were equipped with silicon detectors allowing for precise vertex reconstruction and thus for heavy-flavor jet tagging ("b-tagging") with secondary vertex algorithms. They covered pseudorapidities of up to $|\eta| \sim 2$ for leptons, $|\eta| \sim 4$ for light-flavor jets, and $|\eta| \sim 2$ for heavy-flavor jets. The two Collaborations have been continuously analyzing the acquired data for measurements in all areas of particle physics, including Standard Model (SM) tests, precision measurements of SM parameters, and searches for new physics [1].

Studies of the strong interaction using the Tevatron data are complementary to those using LHC data in the same kinematic regions. The main reason is the different initial state. At the Tevatron, the $p\overline{p}$ initial state favors contributions from processes initiated by valence quarks. For example, in leading order in the strong coupling, vector bosons are mostly produced via $q\overline{q}$ annihilation of valence quarks. This is an advantage, since the parton density functions (PDF) for valence quarks have smaller uncertainties than those for gluons and sea quarks. At the LHC, on the other hand, the pp initial state and the higher collision energy favor contributions from processes initiated by gluons and sea quarks. For example, in leading order, vector bosons are produced either via $q\overline{q}$ annihilation where the antiquark comes from the sea or via Compton-like quark-gluon scattering, while gluon fusion, although of higher order, is also important due to the high gluon luminosity at the LHC energies.

Calculations based on QCD theory can be generally grouped in three types: perturbative calculations of parton-level processes at a fixed order in the strong coupling; parton-shower calculations including hadronization models of the partons; and calculations of parton-level processes resummed to all orders at some logarithmic accuracy over soft gluon emission, and then matched to a fixed-order calculation of the hard scattering process. Fixed-order calculations at next-to-leading order (NLO) are available for all V+jets production process, where V stands for a vector boson (photon, Z or W). An undergoing effort for full next-to-next-to-leading order (NNLO) calculations started with the diphoton production. Parton-shower calculations, effectively performing resummation at leading logarithmic accuracy, started long ago with leading-order (LO) matrix elements. They now have advanced to include higher-order

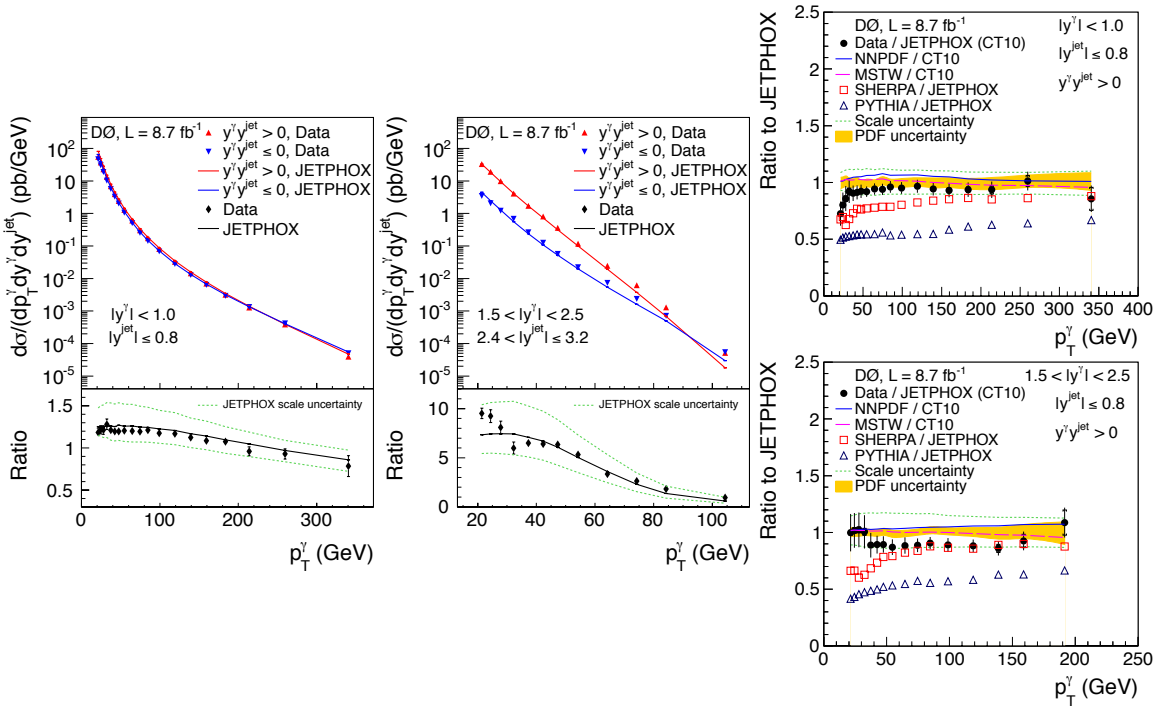

Figure 1: Measured and predicted photon+jet production cross section as a function of the photon transverse momentum for central (left) and forward (middle) photons. The bottom panels of the left and middle plots show the ratios of the measured cross section to the JETPHOX prediction. The plots on the right show the ratios of the measured cross section and various other predictions to the JETPHOX prediction.

matrix elements at the "tree" level (represented by diagrams without loops) and full NLO matrix elements matched to showering and hadronization models. Calculations of this type provide realistic event representations at the particle (hadron) level, typically including an underlying event model for additional parton activity in a hadonic collision, besides the hard parton scattering, and are thus suitable for simulations with detailed detector models. Finally, there exists an extensive phenomenology for non-perturbative QCD, including long-range matrix elements, diffractive models, and underlying event models.

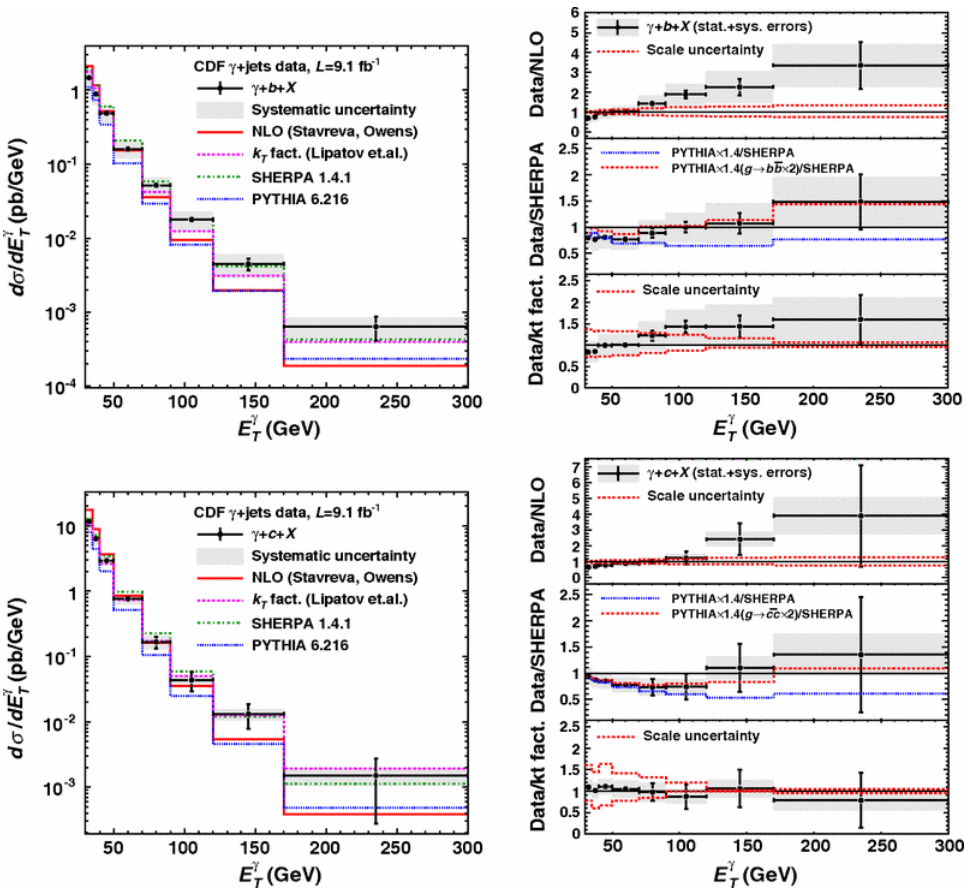

Figure 2: Measured and predicted cross section as a function of the photon transverse energy for photon+b quark (top) and photon+c quark production (bottom). The right plots show the ratios of the measured cross section to various predictions.

2 Prompt photon production

The DZero Collaboration measured the cross section for prompt isolated photon production in association with light-flavor jets [2]. The cross section for photon plus one jet production, differential in the photon transverse momentum p_T^γ, is shown in Figure 1. It is presented for central photons and jets (with absolute rapidities $|y^\gamma| < 1.0$ and $|y^{\rm jet}| \leq 0.8$) in the left window and for forward photons and jets (with $1.5 < |y^\gamma| < 2.5$ and $2.4 < |y^{\rm jet}| \leq 3.2$) in the middle window. In both regions, the cases of the photon and jet emitted close to each other ($y^\gamma y^{\rm jet} > 0$) and away from each other ($y^\gamma y^{\rm jet} \leq 0$) are considered separately, as they probe different parton x ranges. The difference is more important in the forward region. The measurements are compared with predictions of the fixed-order NLO program JETPHOX [3]. This program also implements a phenomenological fragmentation model handling

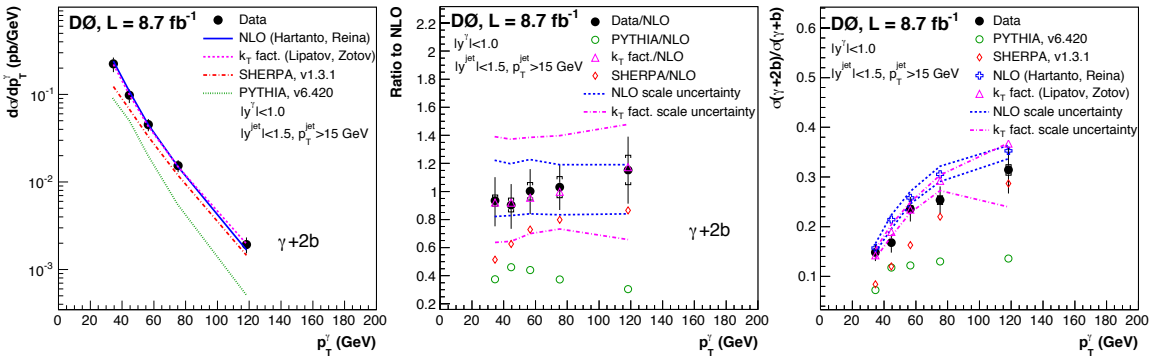

Figure 3: Measured and predicted photon+2b quark production cross section (left), and ratios of the measured cross section to the NLO prediction (middle) and to the measured photon+b quark production cross section (right) as a function of the photon transverse momentum.

the collinear photon emission from final state partons, which causes a singularity in the fixed-order cross section calculation. The description of the data by JETPHOX is generally successful within uncertainties. In the right window, the ratio of the data to the JETPHOX prediction for central jets and central (top) or forward (bottom) photons is compared with the ratios of tree-level parton-shower calculations to JETPHOX. The sensitivity to the PDF choice is also examined. While the JETPHOX prediction agrees with the data within uncertainties, except in the very low p_T^γ region, the parton-shower calculations generally underestimate the data.

The CDF Collaboration measured the cross section for prompt isolated central photon production in association with a heavy-flavor quark [4], charm or bottom. The cross section, differential in the photon transverse energy E_T^γ, is shown in Figure 2. In the left window, the absolute cross section for photon+b quark (top) and photon+c quark production (bottom) is displayed. In the right window, the corresponding ratios of the measured cross section to various theoretical predictions are displayed, for better visualization of the comparisons between data and theory. The analytically resummed "k_T-factorization" calculation [5] and the parton-shower SHERPA calculation [6] agree with the data within uncertainties, whereas the fixed-order NLO calculation fails to describe the data.

An extension of the previous measurement comes from DZero, who measured

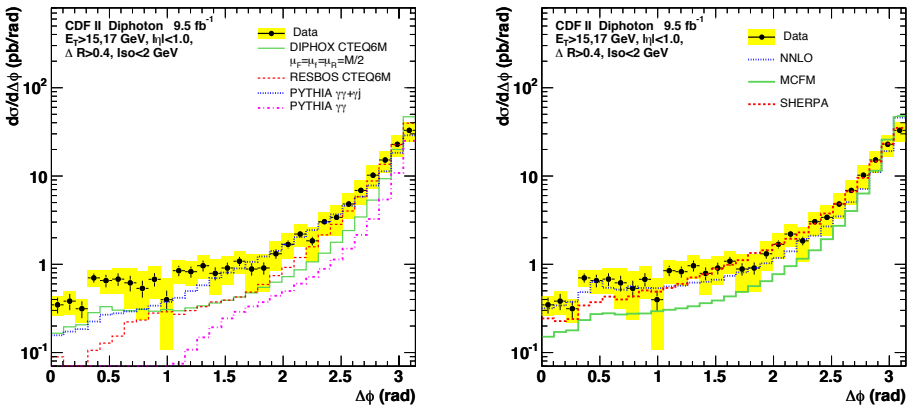

Figure 4: Measured and predicted cross section for photon pair production as a function of the azimuthal angle between the two photons in the event.

the cross section for prompt isolated central photon production in association with two b quarks [7]. Figure 3 shows the cross section, differential in p_T^γ, measured and predicted by various calculations. The cross section is displayed in the left window. The ratios of measured and predicted cross sections to the fixed-order NLO prediction are displayed in the middle window. The ratios of the photon+2b cross section to the photon+b cross section [8] for the data and the various predictions are displayed in the right window. In this case, parton-shower calculations fail to describe the data, whereas the fixed-order NLO and k_T-factorization calculations agree with the data within uncertainties.

CDF measured the cross section for prompt isolated central photon pair production [9]. The measured cross section was studied as a function of a large set of different kinematic variables, sensitive to different details of the diphoton production mechanism, and compared with a variety of state-of-the-art predictions, including parton-shower, fixed-order, and analytically resummed calculations matched to fixed-order NLO terms. Figure 4 shows a characteristic cross section spectrum, differential in the azimuthal distance $\Delta\phi$ between the two photons in the event, compared with various predictions. Only the highest-order calculations, the full fixed-order NNLO calculation [10] and the parton-shower SHERPA calculation with up to three additional jets at the tree level, can reproduce reasonably well the entire spectrum. Similar observations in diphoton production were later made by DZero [11]. This measurement

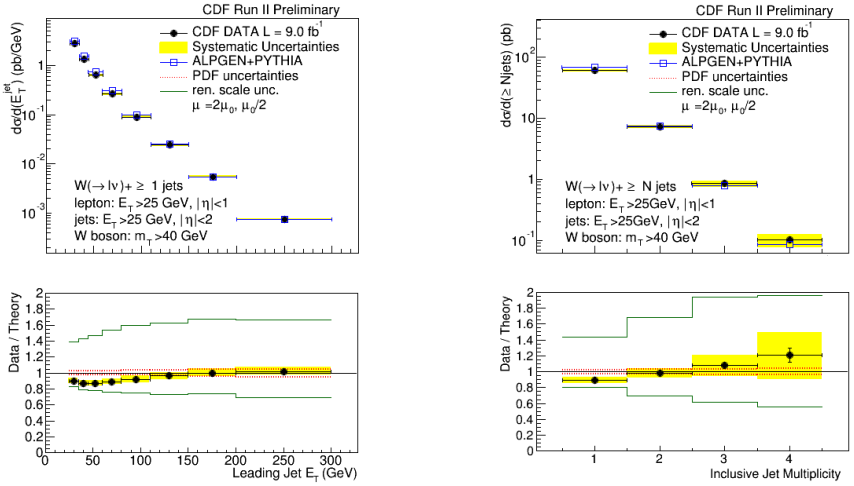

Figure 5: Measured and predicted cross section for W+jets production as a function of the leading jet transverse energy (left) and of the number of jets in the event (right). The bottom panels show the corresponding ratios of the measurement to the prediction.

was the first to test a full NNLO calculation of a QCD process.

3 Weak boson plus jets production

CDF measured the cross section for W boson production in association with light-flavor jets [12], with the W boson reconstructed from the leptonic decays W$\to$eν_e and W$\to\mu\nu_\mu$. In this measurement, particular emphasis was given to the understanding of backgrounds associated with W+jets production and the jet energy corrections required to achieve a good agreement between data and simulations. Figure 5 shows the measured and predicted cross section as a function of the leading jet transverse energy (left window) and the inclusive jet multiplcity (right window). The parton-shower calculation with up to four jets at the tree level, multiplied by a K-factor of 1.4 to account for loop corrections, describes the data well within uncertainties.

DZero measured the cross sections for the production of a W boson in association with a heavy-flavor quark [13], charm or bottom, with the W boson recosntructed only from W$\to\mu\nu_\mu$ decays. These processes are significant backgrounds in many searches for new physics and precision SM measurements. The test of their description by theory is, therefore, important. Figure 6 shows the measured and predicted cross

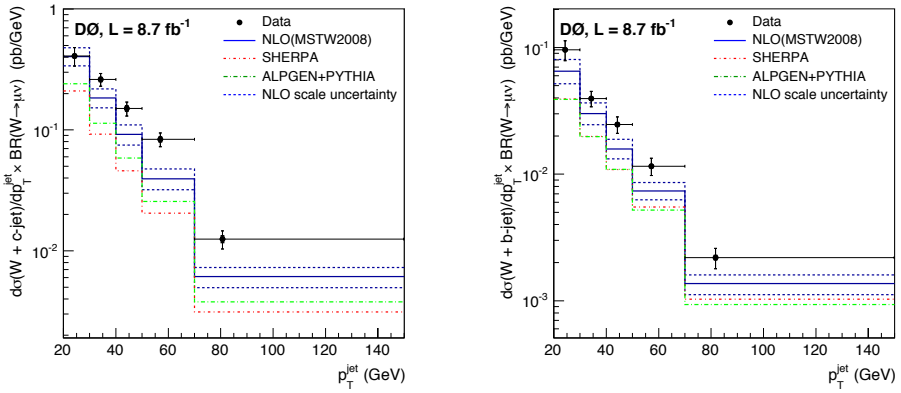

Figure 6: Measured and predicted cross section for W+c quark production (left) and W+b quark production (right) as a function of the transverse momentum of the jet produced by the heavy quark.

sections in the top panel and the corresonding ratios to the NLO predictions in the bottom panel. Neither the tree-level parton-shower calculations nor the fixed-order NLO calculation describe the data adequately. All calculations underestimate the measured cross sections.

CDF measured the cross section for the production of a Z boson in association with light-flavor jets [14]. The Z boson was reconstructed from the leptonic decays Z→ee and Z→$\mu\mu$. The Z+jets production is also an important background in searches and precision measurements. In this measurement, the cross section for various jet multiplicities, differential in many kinematic variables sensitive to different aspects of the production mechanism, was studied in detail and compared with a variety of state-of-the-art calculations. These include tree-level and full NLO matched to parton-shower calculations, parton-level calculations at higher order, and fixed-order calculations at NLO both in the strong and electroweak couplings. Figure 7 provides an example of the cross section as a function of the reconstructed tranverse momentum of the Z boson and the ratios of the measured cross section to various predictions. In the overall, the calculations describe the data adequately, within experimental and theoretical uncertainties.

DZero measured the cross sections for Z boson production in association with a heavy-flavor jet [15], originating from a charm or a bottom quark, normalized to the

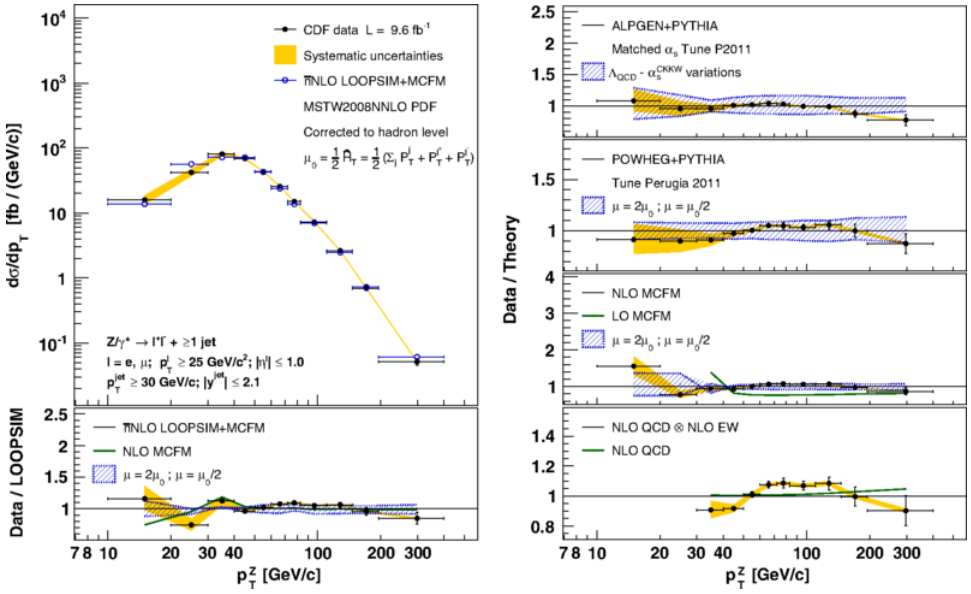

Figure 7: Measured and predicted cross section for Z+jets production as a function of the reconstructed Z boson transverse momentum (top left). The bottom left and the right panels show the ratios of the measured cross section to various predictions.

	Υ+W	Υ+Z
Expected limit (pb)	5.6	13
Observed limit (pb)	5.6	21
Run I observed limit (pb)	93	101

Table 1: Limits on Υ+weak boson production total cross sections.

cross section for Z boson production associated with a light-flavor jet. The Z boson was reconstructed from the leptonic decays Z→ee and Z→$\mu\mu$. Some uncertainties cancel out in the cross section ratios. Figure 8 shows the results compared with various predictions as a function of the reconstructed transverse momentum of the Z boson (left windows) and of the jet (right windows) for a c-jet (top panel) and a b-jet (bottom panel). In general, the theory describes reasonably well the Z+b-jet data, but not the Z+c-jet data.

4 Non-perturbative QCD processes

A class of processes of interest to study is characterized by low momentum transfers in interactions among high-momentum partons. Such processes are important for the

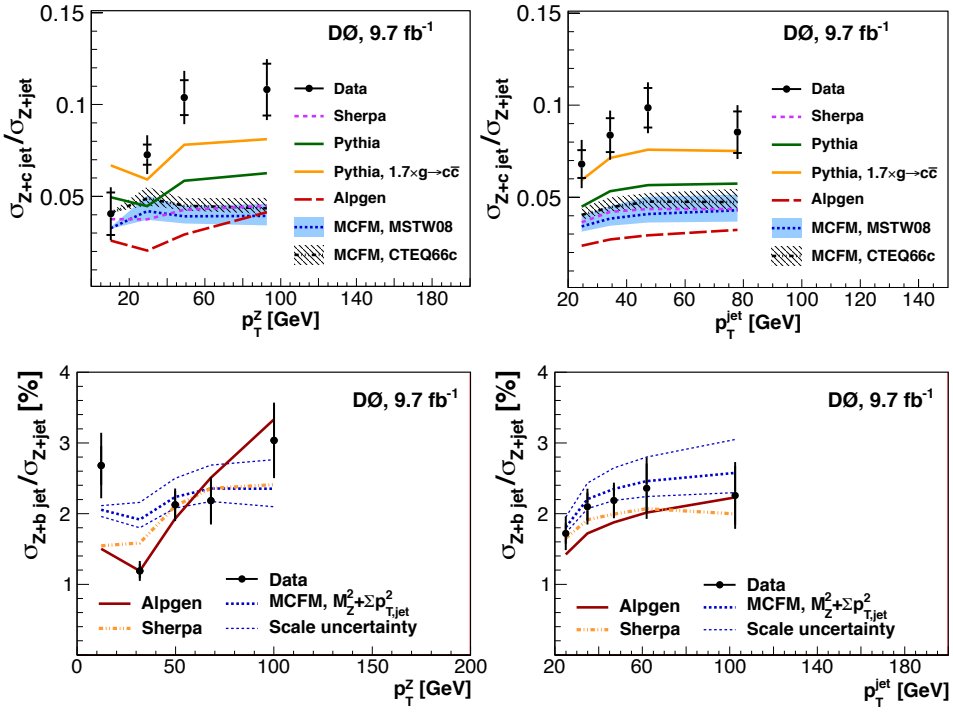

Figure 8: Ratios of cross sections for Z+c (top) and Z+b quark production (bottom) to the Z+jet production cross section as a function of the Z boson transverse momentum (left) and of the jet transverse momentum (right).

understanding of the role of non-perturbative QCD in high-energy hadron collisions. They typically involve the production of low-momentum isolated hadrons, where either the matrix element for the formation of a QCD bound state ("long-range" matrix element) in a hard scattering process or the phenomenology of an entirely soft scattering process (e.g. diffractive scattering, underlying event activity) plays the dominant role.

CDF measured the cross section for the production of a leptonically decaying weak boson, W or Z, in association with an Υ meson [16] and with a D^* meson [17]. In each measurement, of interest is the production mechanism of heavy flavor at low transverse momentum. Table 1 shows the observed and SM expected limits on the Υ+W and Υ+Z production cross sections, compared with the corresponding observed limits from Run I. Although the experiment did not finally reach the statistical power to resolve the SM prediction from a possible anomalous cross section due to new physics, the only so far existing limits from CDF Run I are now improved by an order of magnitude. Figure 9 shows the measured and predicted cross section for W+D^* production as a function of the reconstructed transverse momentum of the D^* meson. The parton-shower calculation, with a LO matrix element for W production and the

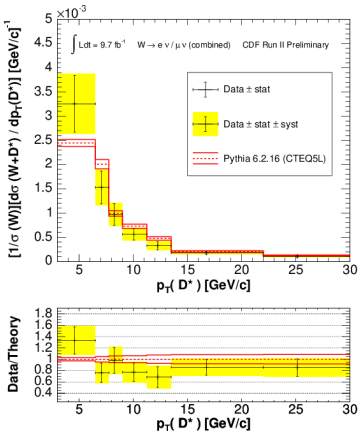
∫Ldt = 9.7 fb⁻¹ W → e ν / μ ν (combined) CDF Run II Preliminary
Data ± stat
Data ± stat ± syst
Pythia 6.2.16 (CTEQ5L)
[1/σ (W)][dσ (W+D*) / dp_T(D*)] [GeV/c]⁻¹
p_T(D*) [GeV/c]
Data/Theory
p_T(D*) [GeV/c]

Figure 9: Measured and predicted cross section for W+D* production as a function of the D* meson transverse momentum. The lower panel shows the ratio of the measurement to the prediction.

D* production modeled through the showering and hadronization prescriptions of the calculation, describes the data well within uncertainties.

DZero is conducting a suite of measurements aiming to study multiple parton interactions in hadron collisions [18]. The strategy is based on analyses of events with 4-body final states, looking into decorrelations of the two pairs of objects ordered in transverse momentum. The analyses look at kinematic variables sensitive to these decorrelations. An example is the azimuthal angle ΔS in the plane normal to the colliding beams between the transverse momentum vectors of the pair of the hardest (highest transverse momentum) reconstructed objects and the pair of the softest (lowest transverse momentum) reconstructed objects. For correlated pairs, this angle tends to be large, as a result of the transverse momentum balance between two pairs originating from a single parton (SP) interaction. For uncorrelated pairs, it tends to be random, signifying that the two pairs originate from double parton (DP) scattering, where the two parton interactions are nearly independent. Figure 10 shows the measured and predicted event distributions for photon+3 jets events (left window) and for 2 photons+2 jets events (right window) as a function of ΔS. The predictions agree well with the data, showing that mutliple parton interactions are understood in these processes.

CDF has performed a detailed program of underlying event (UE) studies. The strategy of this program involves the measurement of inclusive distributions of particles emerging in directions away from the transverse momentum vectors of hard dijets, which are then used to tune phenomenological UE models. In the last mea-

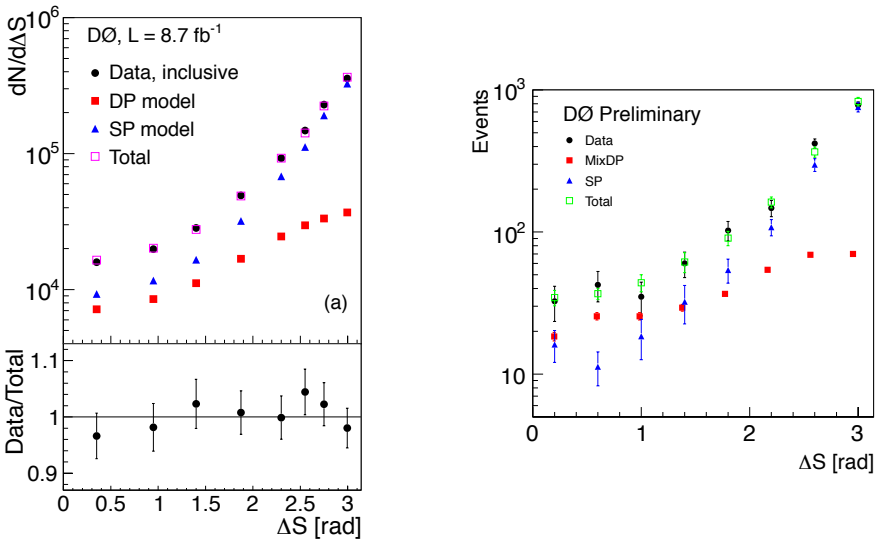

Figure 10: Measured and predicted event distributions for photon+trijet (left) and diphoton+dijet (right) production as a function of the azimuthal separation between the leading and subleading pair of objects in the 4-body final state. The bottom left panel shows the ratio of the measured distribution to the total prediction.

surement [19], the UE dependence on the collision energy was studied using the full luminosity from all three Run II collision energies of 300, 900, and 1960 GeV. Figure 11 shows the measured and modeled densities of charged particles (left window) and their summed transverse momentum (right window) for particles emitted away from the jets. With the appropriate "tune Z1" of the PYTHIA event generator [20], the UE model describes the measured density distributions reasonably well within uncertainties.

Finally, CDF is pursuing a program of measurements of exclusive hadron production in events with only an even number of low-momentum central isolated tracks [21]. Such events are diffractive, characterized by large gaps with no particles produced at large pseudorapidities, and they are sensitive to t-channel double pomeron exchange. This program also exploits the three Run II collision energies. Figure 12 shows the invariant mass distribution of charged pion pairs in the full measured range for 900 and 1960 GeV collision energy (left window) and in the high-mass range for the 1960 collision energy (right window), where the statistics is significant. The low-mass peak originates from the $f_2(1270)$ and $f_0(1370)$ mesons decays, while more structure is visible in the high-mass tail. The program probes a so far entirely unexplored region of soft QCD.

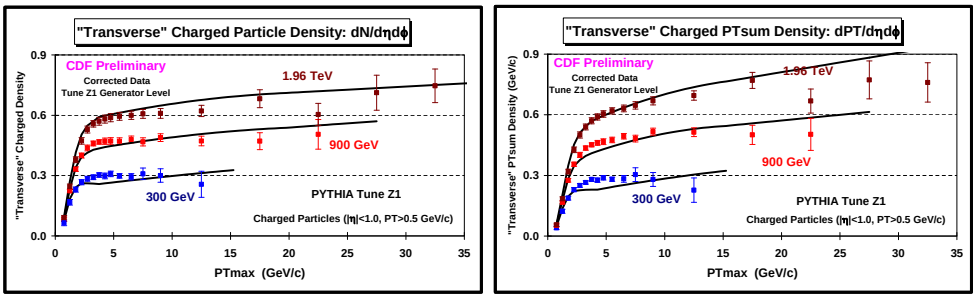

Figure 11: Measured and predicted inclusive particle densities as a function of the maximum single-object transverse momentum in the event.

5 Conclusions

The Tevatron experiments, CDF and DZero, continue producing high-precision results that provide stringent constraints of QCD calculations. The experimental precision challenges the precision of NLO calculations in most cases. NNLO calculations are generally needed to adequately describe processes involving prompt photon production. W/Z+jets measurements, in general, are successfully described by NLO calculations within experimental and theoretical uncertainties, with the exception of W boson production in association with heavy flavor quarks. Multiple parton interactions are reasonably well understood. Long-range matrix elements and diffractive physics are probed more precisely with the full luminosity data. The variety of collision energies reached in the end of Run II allows for the study of the energy dependence of non-perturbative QCD effects in certain cases.

References

[1] Links to all public results from the Tevatron experiments can be found at http://www-cdf.fnal.gov/physics/physics.html and http://www-d0.fnal.gov/Run2Physics/WWW/results.htm.

[2] V.M. Abazov *et al.* (DZero Collaboration), Phys. Rev. D **88**, 072008 (2013).

[3] S. Catani, M. Fontannaz, J.-Ph. Guillet, and E. Pilon, J. High Energy Phys. 2002, 05 (2002).

[4] T. Aaltonen *et al.* (CDF Collaboration), Phys. Rev. Lett. **111**, 042003 (2013).

[5] A.V. Lipatov, M.A. Malyshev, and N.P. Zotov, J. High Energy Phys. 05, 104 (2012).

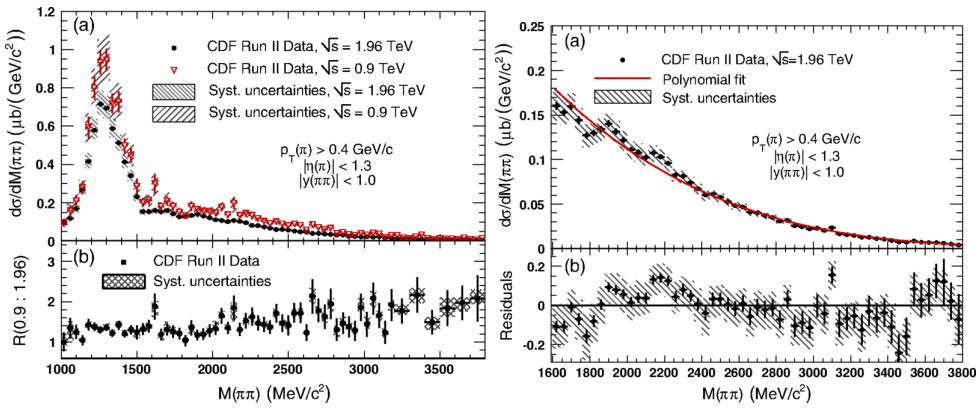

Figure 12: Measured cross section for exclusive central pion pair production at two collision energies as a function of the invariant mass of the pair for the full mass range at both energies (left) and the high mass range at the highest energy (right). The bottom left panel shows the difference between the cross sections at the two energies. The bottom right panel shows the residuals of the cross section at the highest energy from an empirical polynomial fit.

[6] T. Gleisberg, S. Hoche, F. Krauss, M. Schonherr, S. Schumann, F. Siegert, and J. Winter, J. High Energy Phys. 02, 007 (2009).

[7] V.M. Abazov *et al.* (DZero Collaboration), Phys. Lett. **B** 737, 357 (2014).

[8] V.M. Abazov *et al.* (DZero Collaboration), Phys. Lett. **B** 714, 32 (2012); Phys. Lett. **B** 179, 354 (2012).

[9] T. Aaltonen *et al.* (CDF Collaboration), Phys. Rev. Lett. **110**, 101801 (2013).

[10] S. Catani, L. Cieri, D. de Florian, G. Ferrera, and M. Grazzini, Phys. Rev. Lett. **108**, 072001 (2012).

[11] V.M. Abazov *et al.* (DZero Collaboration), Phys. Lett. **B** 725, 6 (2013).

[12] T. Aaltonen *et al.* (CDF Collaboration), CDF conference note 11167.

[13] V.M. Abazov *et al.* (DZero Collaboration), Phys. Lett. **B** 743, 6 (2015).

[14] T. Aaltonen *et al.* (CDF Collaboration), Phys. Rev. D **91**, 012002 (2015).

[15] V.M. Abazov *et al.* (DZero Collaboration), Phys. Rev. D **87**, 092010 (2013); Phys. Rev. Lett. **112**, 042001 (2014).

[16] T. Aaltonen *et al.* (CDF Collaboration), Phys. Rev. D **91**, 052011 (2015).

[17] T. Aaltonen *et al.* (CDF Collaboration), CDF conference note 11087.

[18] V.M. Abazov *et al.* (DZero Collaboration), Phys. Rev. D **89**, 072006 (2014); D0 conference note 6470.

[19] T. Aaltonen *et al.* (CDF Collaboration), CDF conference note 10874.

[20] T. Sjöstrand, S. Mrenna, and P. Skands, J. High Energy Phys. 2006, 05 (2006).

[21] T. Aaltonen *et al.* (CDF Collaboration), Phys. Rev. D **91**, 091101 (2015).